frontiers in Energy Research

ORIGINAL RESEARCH
published: 12 April 2021
doi: 10.3389/fenrg.2021.663270

Polyether-Based Supramolecular Electrolytes With Two-Dimensional Boroxine Skeleton

Masahiro Yoshizawa-Fujita, Shunsuke Horiuchi, Tamao Uemiya, Jun Ishii, Yuko Takeoka and Masahiro Rikukawa*

Department of Materials and Life Sciences, Sophia University, Chiyoda, Japan

Solid polymer electrolytes mainly based on polyethers have been actively investigated for over 40 years to develop safe, light, and flexible rechargeable batteries. Here, we report novel supramolecular electrolytes (SMEs) composed of polyether derivatives and a two-dimensional boroxine skeleton synthesized by the dehydration condensation of 1,4-benzenediboronic acid in the presence of a polyether with amines on both chain ends. The formation of SMEs based on polyether derivatives and boroxine skeleton was confirmed by Fourier transform infrared (FT-IR) spectroscopy, X-ray photoelectron spectroscopy (XPS), powder X-ray diffraction (PXRD), and thermogravimetric (TG) analysis. Linear sweep voltammetry (LSV) and cyclic voltammetry (CV) were performed to evaluate the electrochemical stability and lithium conductive properties of SMEs with given amounts of lithium bis(trifluoromethylsulfonyl)amide (LiTFSA). The ionic conductivity of SME/LiTFSA composites increased with increasing lithium-salt concentration and reached a maximum value at a higher concentration than those of simple polyether systems. The lithium-ion transference number (t_{Li+}) of SME/LiTFSA was higher than those of polyether electrolytes. This tendency is unusual for a polyether matrix. SME/LiTFSA composite electrolytes exhibited a stable lithium plating/striping process even after 100 cycles. The current density increased with an increasing number of cycles. The combination of ion conductive polymers and a two-dimensional boroxine skeleton will be an interesting concept for developing solid electrolytes with good electrochemical properties.

Keywords: supramolecular, solid polymer electrolytes, boroxine, covalent organic frameworks, lithium-ion batteries

OPEN ACCESS

Edited by:
Jun Mei,
Queensland University of Technology, Australia

Reviewed by:
Makoto Moriya,
Shizuoka University, Japan
Lu Han,
Oak Ridge National Laboratory (DOE), United States
Qian Zhang,
Taiyuan University of Technology, China

****Correspondence:***
Masahiro Yoshizawa-Fujita
masahi-f@sophia.ac.jp

Specialty section:
This article was submitted to Electrochemical Energy Conversion and Storage, a section of the journal Frontiers in Energy Research

Received: *02 February 2021*
Accepted: *23 March 2021*
Published: *12 April 2021*

Citation:
Yoshizawa-Fujita M, Horiuchi S, Uemiya T, Ishii J, Takeoka Y and Rikukawa M (2021) Polyether-Based Supramolecular Electrolytes With Two-Dimensional Boroxine Skeleton. Front. Energy Res. 9:663270. doi: 10.3389/fenrg.2021.663270

INTRODUCTION

Lithium-ion batteries (LIBs) have been rapidly developed over the past three decades. As a result, LIBs are widely being used in many applications such as laptops, mobile phones, electric vehicles, etc. (Armand and Tarascon, 2008). However, their safety and energy density must be improved for further expanding the use of LIBs. Currently, organic liquid electrolytes (e.g., ethylene carbonate, diethyl carbonate) are employed in LIBs. Although LIBs that employ these conventional liquid electrolytes exhibit good performance, organic liquid electrolytes pose inevitable risks, including leakage and low ignition temperatures. Recently, solid polymer electrolytes (SPEs) have been actively studied as solid electrolytes for developing rechargeable batteries

(Agrawal and Pandey, 2008; Mindemark et al., 2018) because SPEs have advantages over conventional organic liquid electrolytes, such as no leakage, flame retardancy, excellent flexibility, in addition to being lightweight. In addition, SPEs function as a separator. Conventional SPEs are generally prepared by dissolving a lithium salt into a polymer matrix, which in some cases additionally contains plasticizers. The polymer matrix is usually composed of ether oxygen (Armand, 1986; Meyer, 1998), carbonate (Okumura and Nishimura, 2014; Sun et al., 2014; Tominaga and Yamazaki, 2014), and ketone (Eriksson et al., 2020) (Lewis base) functionalities to solvate Li^+. The generated Li^+ cations in the polymer matrix are transported along the polymer backbone and/or segments through the interactions between Li^+ cations and units of Lewis base.

Among various ion conductive polymers, ether oxygen atoms are an important component because they effectively solvate ions and transport ions along the polymer backbone (vide supra). Although many poly(ethylene oxide) (PEO) derivatives have been reported, it is inherently difficult to achieve both high ionic conductivity and Li^+ transference number. Modifying the ethylene oxide backbone with other functional groups is an interesting methodology for reducing the crystallinity, a property that retards ion transport properties in the PEO framework. Poly(propylene oxide) (PPO), which is structurally similar to PEO, is an amorphous material. Thus, the copolymers of PEO and PPO (P(EO-*co*-PO) reduce the crystallinity of PEO and create amorphous regions in the matrix (Liang et al., 2004; Tien et al., 2008). Furthermore, P(EO-*co*-PO)s have strong dipole moments to solvate ions.

PEO-based electrolytes with various lithium salts have been investigated for improving their electrochemical properties. Such lithium salts usually include anions with a weakly coordinating nature, such as hexafluorophosphate (PF_6^-) (Magistris et al., 2000), triflate ($CF_3SO_3^-$) (Appetecchi et al., 2003; Karan et al., 2008), bis(trifluoromethylsulfonyl)amide ($[N(SO_2CF_3)_2]^-$, $TFSA^-$) (Lascaud et al., 1994; Marzantowicz et al., 2005), bis(pentafluoroethylsulfonyl)amide ($[N(SO_2C_2F_5)_2]^-$, $BETA^-$) (Appetecchi et al., 2001, 2005), and so on. LiTFSA has been most actively studied as the electrolyte salt for SPEs due to three intrinsic features of $TFSA^-$. The first feature is the highly delocalized charge distribution of $TFSA^-$, which induces the dissociation of LiTFSA in polymer matrices, thus producing a large amount of carrier ions. The second feature is the high flexibility of the -S-N-S- bond of $TFSA^-$, which results in reducing the crystallinity of polymer matrices. The third feature is excellent thermal and electrochemical stabilities, which are suitable for stable electrolyte materials. These important features of $TFSA^-$ are useful for developing SPEs for Li-ion batteries and other electrochemical devices (Yue et al., 2016).

On the other hand, covalent organic frameworks (COFs) are highly porous, high surface area crystalline materials composed of light elements (C, H, N, B, and O) (Côté et al., 2005). These unique features have produced much interest in using COFs for gas storage (Côté et al., 2007; Klontzas et al., 2010) and battery application (Yang et al., 2016; Lei et al., 2018; Li et al., 2020). For example, a framework structure (COF-1) is formed as a result of self-condensation of 1,4-benzenediboronic acid as shown in **Figure 1**. All boron atoms are three-coordinated to a phenyl ring and two oxygen atoms in a defect-free structure. These COF materials have high thermal stability, but even slightly humid air will cause decomposition to the boronic acid starting materials due to nucleophilic attack by water at the electron-deficient boron sites (Lanni et al., 2011). Such problem is a major limitation to the use of COFs with boroxine skeleton for many applications. In a previous study, Du et al. (2013) reported that COFs with pyridine were stabilized by formation of B-N bonds. The lone pair electrons of the nitrogen atom interact strongly with the vacant p-orbital of the boron atom. In other words, coordination bonds are generated between the boron of the boroxine as the Lewis acid and the nitrogen of the amine as the Lewis base. The resulting coordination may in some cases improve the stability of boroxine rings (Du et al., 2014).

In this study, we synthesize supramolecular electrolytes by combining COF-1 and a commercially available P(EO-*co*-PO) copolymer with amines on both chain ends (Jeffamine® ED-2003), here-after referred to as ED-2003. It is expected that the boroxine rings of COF-1 will function as the cross-linking points, and ED-2003 will serve as the cross-linker. As a result, supramolecular electrolytes will be formed. Furthermore, the boroxine ring is expected to function not only as the cross-linking point but also an anion receptor site through the coordination bond between electron-rich anion and vacant p-orbital of boron atom. Anion trapping polymer electrolytes with boroxine rings and organoboron compounds have been reported (Mehta et al., 1999; Matsumi et al., 2003, 2005) and exhibit high Li^+ transference numbers of over 0.6.

EXPERIMENTAL

Materials

1,4-Benzenediboronic acid (BDBA) and dehydrated 1,4-dioxane (>99.5%) were purchased from Tokyo Chemical Industry Co., Ltd. Dehydrated 1,3,5-mesitylene was purchased from Sigma-Aldrich. Polyether with diamines, Jeffamine® ED-2003 (Huntsman, $M_n = 2000$), was dried *in vacuo* at 60°C prior to use. Lithium bis(trifluoromethylsulfonyl)amide (LiTFSA, Kanto Chemical Industry Co., Ltd) was dried *in vacuo* prior to use. Li foils (thickness: 0.4 mm, diameter: 16 mm) were purchased from Honjo Metal Co., Ltd.

Synthesis of Supramolecular Electrolytes

The synthesis of COF-1/ED-2003 complex as a SME is shown in **Figure 2**. BDBA (0.25 g, 1.51 mmol) and ED-2003 (3.00 g, 1.50 mmol) were mixed in a flask filled with 1,3,5-mesitylene/1,4-dioxane (1/1 *v*/*v*, 6 mL). The suspension was stirred at 90°C for 15 min, 100°C for 15 min, and then 120°C for 20 min. The resulting gel-like compound was collected by filtration. After washing the gel-like compound with dehydrated acetone (three times), the complex was obtained as a white powder in 80% yield.

Preparation of LiTFSA Composites

SME/LiTFSA composites were prepared by mixing SME and LiTFSA at room temperature in an Ar-filled glove box. The ratio

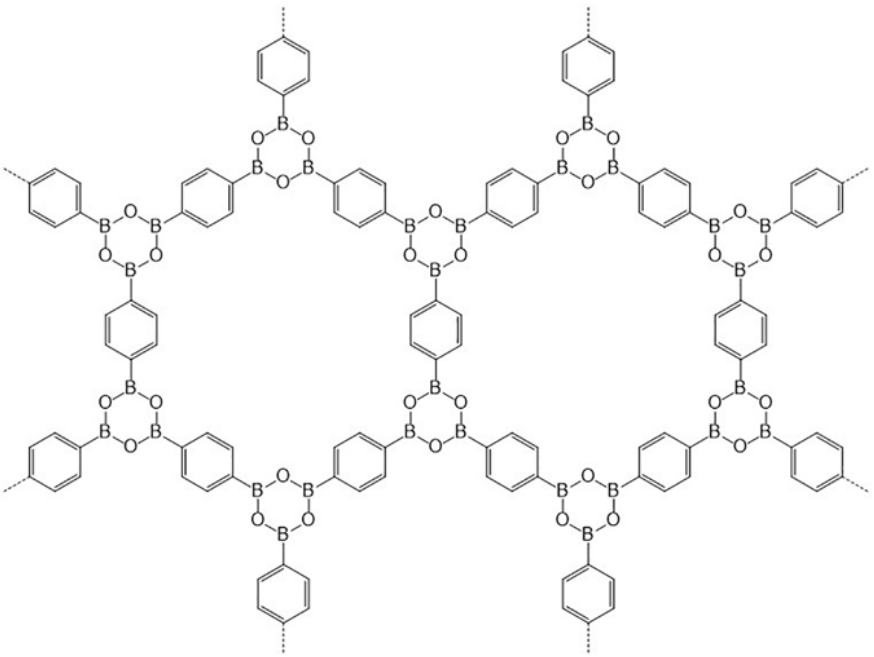

FIGURE 1 | Chemical structure of COF-1.

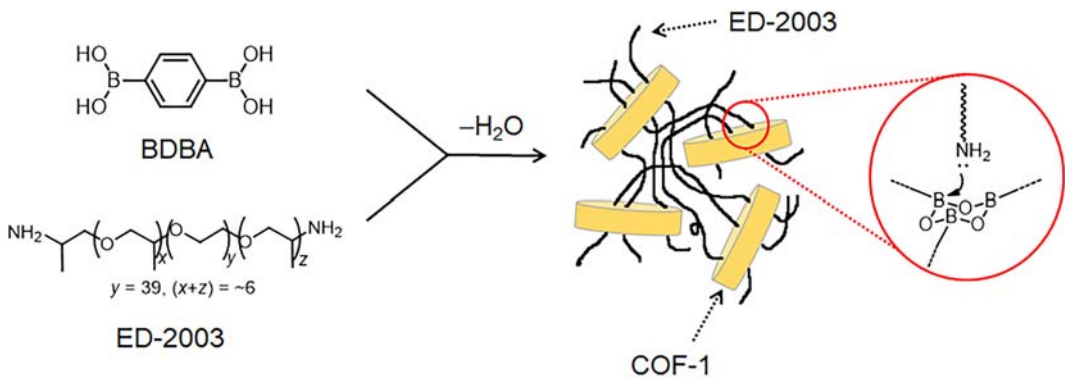

FIGURE 2 | Synthesis of SME based on COF-1 and ED-2003.

of Li^+ and ether oxygen of ED-2003 is denoted as Li/O, and their values are 0.04, 0.08, 0.13, 0.14, 0.17, and 0.20, respectively. After mixing, SME/LiTFSA composites were dried *in vacuo* at 60°C for 24 h prior to use.

Measurements

Fourier transform infrared (FT-IR) spectroscopy was conducted with a Nicolet 6700 FTIR spectrometer (Thermo Fisher Scientific). FT-IR measurements were carried out by the ATR method with a diamond crystal for ED-2003 and SME, and KBr pellet method for BDBA at room temperature. The spectrum was obtained from 4,000 to 650 cm^{-1} with 1 cm^{-1} resolution. XPS analysis was performed with a PHI 5800 Versa Probe spectrometer (ULVAC Phi Inc.). High resolution scans of the B1s and O1s energy spectra were taken with a pass energy of 58.7 eV. The powder X-ray diffraction (PXRD) pattern of the samples was measured on a SmartLab (Rigaku) at room temperature using Cu K_α radiation for 2θ values between 5 and 40°.

The thermal stabilities were studied by thermogravimetric analysis (TGA; TG-DTA7200, Hitachi High-Technologies Corp.). The samples were heated from room temperature to 500°C at a heating rate of 10°C min^{-1} under a N_2 atmosphere. The phase transition behavior of the samples was studied using differential scanning calorimetry (DSC; DSC7020, Hitachi High-Technologies Corp.) between −100 and 150°C at heating/cooling rate of 10°C min^{-1}.

The ionic conductivity values of the samples were obtained by measuring the complex impedance between 50 mHz and 1 MHz (applied voltage: 10 mV) using an impedance analyzer (VSP-300, BioLogic) over the temperature range of 0 to 100°C.

The temperature was controlled using a constant-temperature oven (SU-262, Espec Corp.). A stainless steel cell (TYS-00DM01, Toyo System Co., Ltd.) was used for the measurements. Two platinum plates polished with 1.0, 0.3, and 0.05 μm Al_2O_3 powder were used as the blocking electrode. The AC impedance method was used to analyze the ionic conductivity of the SPE at various temperatures. The ionic conductivity of the electrolytes was determined using

$$\sigma = \frac{d}{RS}$$

where σ represents ionic conductivity, R is the resistance, which is obtained from the intercept at the real axis in the Nyquist plot, S is the area of the electrolyte-electrode interface, and d is the distance between the two electrodes.

To determine the conduction species in SME composites, the lithium-ion transference number (t_{Li+}) was measured using a combination of AC impedance and DC polarization with a symmetric Li/electrolyte/Li cell at 60°C, which was controlled using a constant temperature oven (TB-1, BAS Inc.) (Evans et al., 1987; Watanabe et al., 1988; Abraham et al., 1997). The DC polarization curves (potential bias (DV): 100 mV in this study) of the cells were recorded until a steady current was obtained (about 8 h in this study). The AC impedance spectra of the cells were recorded in the frequency range of 10 mHz and 7 MHz with an oscillation voltage of 10 mV before and after the DC polarization measurement. The t_{Li+} was determined using

$$t_{Li}^{+} = \frac{I_s R_b{}^s(\triangle V - I_0 R_i{}^0)}{I_0 R_b{}^0(\triangle V - I_s R_i{}^s)}$$

where I_0 and I_s are the initial and steady currents, $R_b{}^0$ and $R_b{}^s$ are the initial and final resistances of the electrolyte, and $R_i{}^0$ and $R_i{}^s$ are the initial and final resistances of interfacial layers of the Li metal/electrolyte.

Linear sweep voltammetry (LSV) (VSP-300, BioLogic) was performed at 60°C at a scan rate of 10 mV s^{-1}. Li foils were used as the reference and counter electrodes, while a platinum plate was used as working electrode. Cyclic voltammetry (CV) measurements were carried out in the potential range of −0.25 and 1.0 V at 60°C at a scan rate of 1 mV s^{-1}, with Li foils as the reference and counter electrodes.

RESULTS AND DISCUSSION

Structure Analysis

Fourier transform infrared spectroscopic study was performed to analyze the chemical bonds in SME. **Figure 3** exhibits the FT-IR spectra of BDBA, ED-2003, and SME. BDBA exhibited an asymmetric B-O stretching mode at 1,346 cm^{-1} and symmetric B-C stretching modes at 1,029 and 1,006 cm^{-1} (Côté et al., 2005). The spectrum of ED-2003 exhibited a C-O-C asymmetric stretching vibration mode at 1,103 cm^{-1} and asymmetric CH_2 bending mode at 1,466 cm^{-1} (Wen et al., 1996; Pucić and Jurkin, 2012). Three distinct vibrational modes of boroxine were found to involve the stretching modes of the B-C (aryl) bond, corresponding to 1,347, 1,290, and 1,257 $cm^{-1}$for SME. Two modes of the boroxine ring were also observed at 746 and 696 cm^{-1} (Smith and Northrop, 2014). Both modes are assigned as the out-of-plane bending of boron atoms. The higher frequency mode, 746 cm^{-1}, corresponds to boron displacements

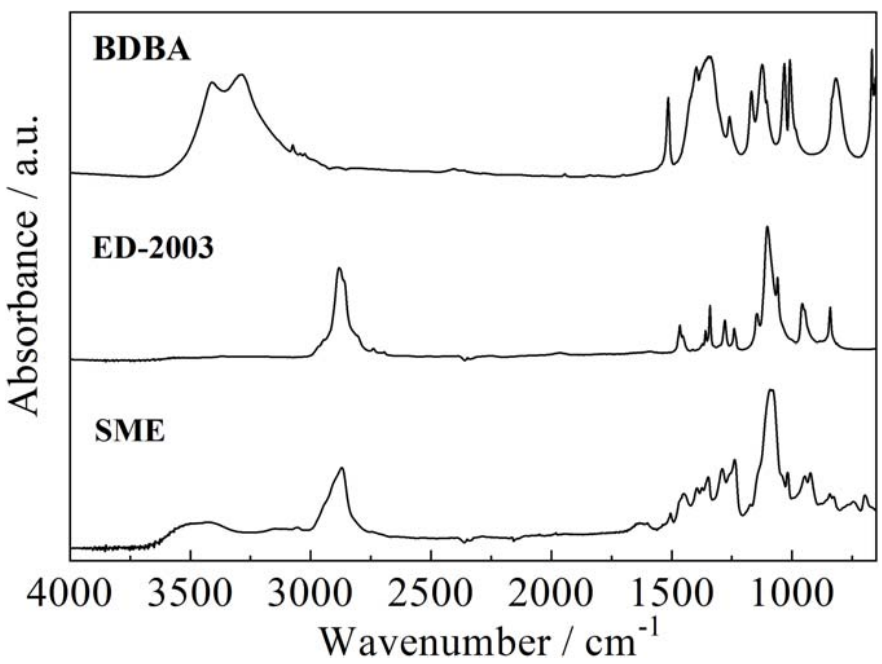

FIGURE 3 | FT-IR spectra of BDBA, ED-2003, and SME.

that are anti to the displacements of aryl hydrogen atoms. The lower frequency mode, 696 cm^{-1}, corresponds to displacements of boron atoms syn to the displacements of aryl hydrogen atoms. Furthermore, the hydroxyl bands of BDBA were absent in SME. The FT-IR spectrum of SME indicated the formation of the boroxine rings in COF-1 and the composite material is comprised of COF-1 and ED-2003.

The O 1s and B 1s XPS spectra for BDBA and SME are depicted in **Figure 4**. The B 1s binding energies do not exhibit significant shifts (see the inset in **Figure 4A**) because the B-C bonds do not change through the condensation. On the other hand, a slight shift of the O 1s binding energy, from 532.2 eV for the starting material, BDBA, to 531.8 eV for the SME, was observed. This tendency is in good accordance with the change of the oxygen chemical environment through the condensation. The oxygen atoms of BDBA are bound to both boron and hydrogen atoms, whereas the oxygen atoms of COF-1 are bound to two boron atoms. As hydrogen atoms are more electronegative than electron-deficient boron atoms, oxygen atoms become more negative in the boroxine rings of COF-1. This results in a slightly lower O 1s binding energy in SME. Comparison reveals that the O 1s binding energy of SME shifted toward a lower value due to the condensation of boronic acid groups into boroxine rings (Dienstmaier et al., 2011).

Powder X-ray diffraction (PXRD) analysis of BDBA, COF-1, ED-2003, and SME confirmed the crystallinity of materials, as shown in **Figure 5**. Côté et al. (2005) reported that COF-1 has two different stacking structures. One is a staggered AB arrangement, similar to the packing of graphite sheets, in which the three connected vertices (carbon atoms) are located at the center of the six-membered rings of the adjacent graphite layers. The other is an eclipsing arrangement, similar to boron nitride, in which the atoms of adjacent sheets are located directly on top of each other (Côté et al., 2005). On the other hand, in the case of ED-2003, it is a crystalline polymer, and there are two main peaks at 19 and 23°. PXRD results revealed no diffraction peaks of SME that could be attributed to starting materials or their known solvates and showed broad peak patterns as shown in **Figure 5**, which is corresponding to the amorphous phase of SME. This should be based on the formation of a three-dimensional network between ED-2003 and two-dimensional COF-1 skeleton.

Thermal Properties

Figure 6 shows TG curves of BDBA, ED-2003, and SME. BDBA exhibited a weight loss of 20% at around 200°C due to the dehydration condensation of BDBA. The pyrolysis residue of BDBA with a large amount of inorganic component was much higher than those of ED-2003 and SME. The temperatures corresponding to the 5% weight loss temperature ($T_{d5\%}$) of ED-2003 and SME were 340 and 310°C, respectively, which are sufficiently high for their application as solid electrolytes of rechargeable batteries. The pyrolysis residue of SME with COF-1 is higher than that of ED-2003 due to the presence of COF-1, which is inorganic component.

The thermal transitions of SME and SME/LiTFSA were investigated by DSC measurements as shown in **Figure 7**. ED-2003 exhibited a melting point (T_m) at 43°C, whereas SME exhibited a glass transition temperature (T_g) at −56°C. The T_m of ED-2003 disappeared after mixing with COF-1. The crystallization of ED-2003 was inhibited by the interaction between ED-2003 and boroxine rings. This result is in good accordance with the XRD pattern of SME, which shows no sharp diffraction peaks. All the SME/LiTFSA composites used in this study exhibited T_g values only. When the LiTFSA concentration was Li/O = 0.04, the T_g of SME/LiTFSA was −47°C, which is 11°C higher than that of SME. The T_g values of SME/LiTFSA composites monotonously increased with increasing Li salt concentration in the range of Li/O = 0.04 and 0.20. This is a typical tendency for polyether-based electrolytes because polyether chains become stiff through the interaction between ether oxygen and Li cation.

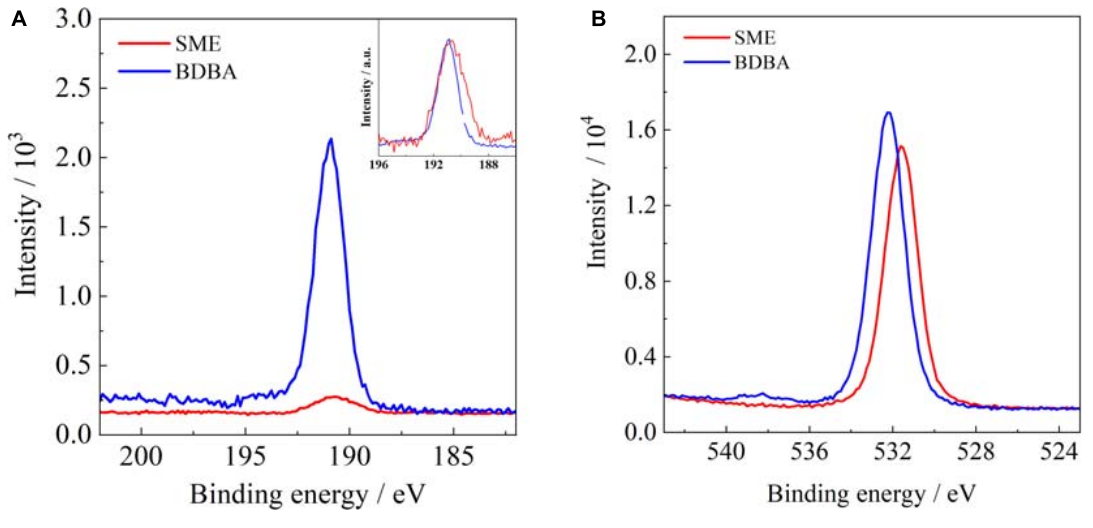

FIGURE 4 | XPS spectra of **(A)** B 1s and **(B)** O 1s core level binding energies in BDBA and SME.

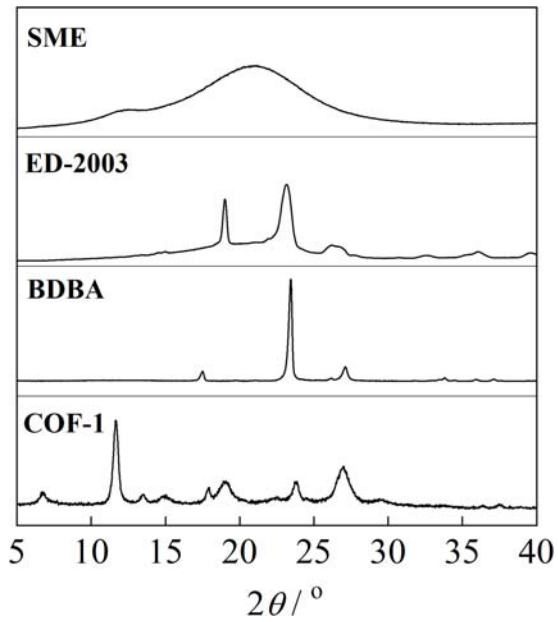

FIGURE 5 | PXRD patterns of BDBA, COF-1, ED-2003, and SME.

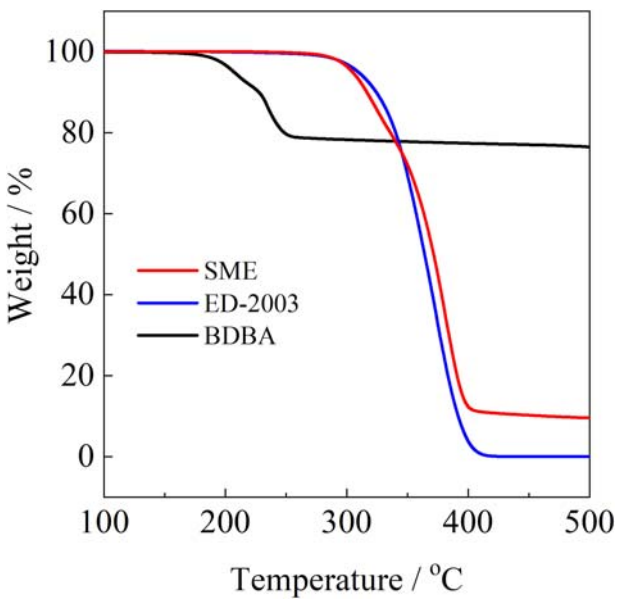

FIGURE 6 | TG curves of BDBA, ED-2003, and SME.

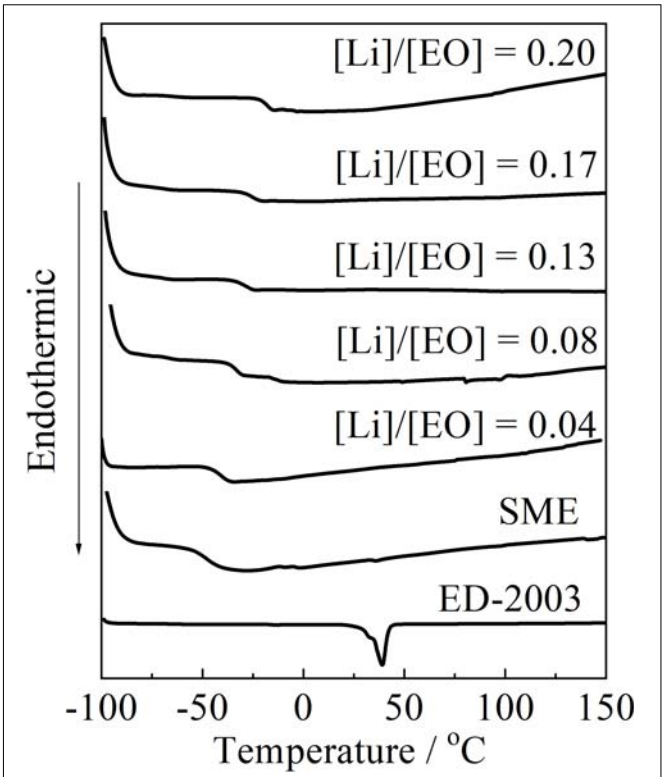

FIGURE 7 | DSC traces of ED-2003, SME, and SME/LiTFSA composites.

Electrochemical Properties

Figure 8 shows Arrhenius plots of ionic conductivities for SME/LiTFSA composites with various Li concentrations. The temperature dependence of ionic conductivities exhibited an upper convex curve for all the SME/LiTFSA composites in the whole temperature range. This suggests that ED-2003, which is the polyether matrix, provides the ion conduction path in SME/LiTFSA composites, and SME/LiTFSA composites are completely amorphous, which is consistent with the results of PXRD and DSC measurements. SME/LiTFSA composites showed ionic conductivities of 10^{-6}–10^{-4} S cm^{-1} at 25°C. In general, PEO/Li-salt electrolytes show poor ionic conductivities (10^{-8}–10^{-6} S cm^{-1}) at temperatures below 40°C due to the crystallization of the PEO matrix (Tominaga and Yamazaki, 2014; Zhang et al., 2014). The crystallinity of ED-2003 was inhibited in the composites. The amorphous ED-2003 will contribute to improve the ionic conductivity of SME/LiTFSA composites at temperatures below 40°C. The ionic conductivity of SME/LiTFSA composites are comparable to those of polycarbonate- and polyester-based electrolytes (Mindemark et al., 2018).

The ionic conductivity maintained almost the same value from Li/O = 0.04 to 0.13. After that, the ionic conductivity values increased with increasing the Li salt concentration. At Li/O = 0.17, SME/LiTFSA showed the highest ionic conductivity value of 9.8×10^{-5} S cm^{-1} at 25°C. This tendency was different from typical polyether-based electrolytes that show the maximum ionic conductivity at around Li/O = 0.05 (Ratner and Shriver, 1988; Tominaga and Yamazaki, 2014). The dissociation of Li salts would be enhanced through the interaction between boroxine rings and TFSA anion. This will contribute to produce a large amount of carrier ions in SME/LiTFSA composites. Mehta et al. (1999) reported that SPE composed of boroxine rings with ethylene oxide side chains showed an ionic conductivity value of 1.6×10^{-5} S cm^{-1} at 30°C when LiTFSA was doped into

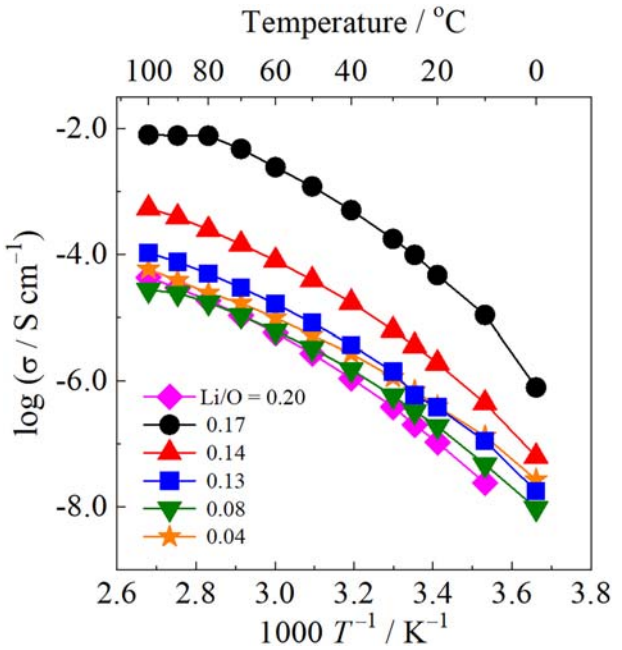

FIGURE 8 | Arrhenius plots of ionic conductivities for SME/LiTFSA composites.

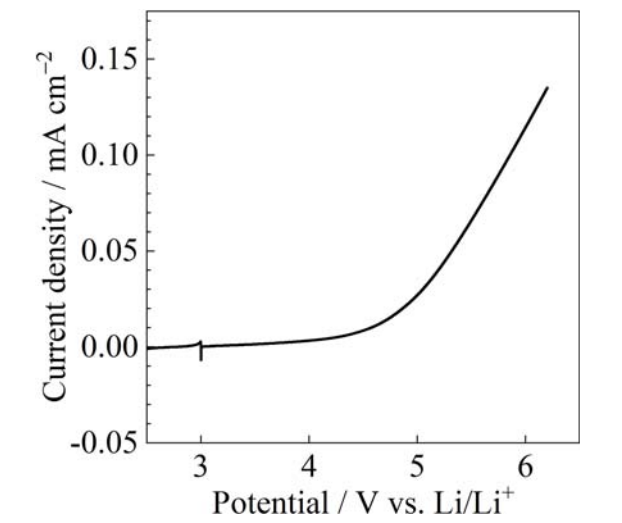

FIGURE 9 | LSV curve of SME/LiTFSA (Li/O = 0.17) at a scan rate of 10 mV s^{-1} at 60°C.

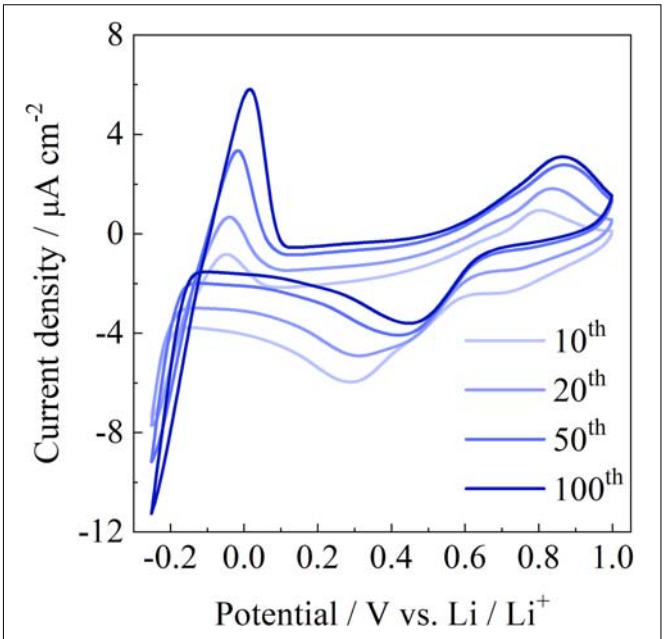

FIGURE 10 | CV curves of SME/LiTFSA (Li/O = 0.17) over 100 cycles at a scan rate of 10 mV s^{-1} at 60°C.

the boroxine-containing SPE. The SME composed of polyether and two-dimensional boroxine skeleton exhibited higher ionic conductivity at room temperature than that of the boroxine-containing SPE.

The lithium-ion transference number (t_{Li+}) of SME/LiTFSA (Li/O = 0.17), which showed the best ionic conductivity among various LiTFSA concentrations, was determined to estimate the conduction species in the composites. The t_{Li+} was measured according to the literature method (Evans et al., 1987; Watanabe et al., 1988; Abraham et al., 1997). SME/LiTFSA (Li/O = 0.17) showed a t_{Li+} of 0.34 at 60°C, which was higher than those of 0.16 (Feng et al., 2013) and 0.18 (Zhang et al., 2014) at 80°C reported for PEO/LiTFSA (Li/O = 0.05). These results clearly indicate that the boroxine rings of COF-1 function as anion receptor sites through the coordination bond between electron-rich anion and the vacant p-orbital of boron atom. But the t_{Li+} of SME/LiTFSA was lower than those of anion trapping polymer electrolytes with boroxine rings and organoboron compounds (Mehta et al., 1999; Matsumi et al., 2003, 2005). This is because the boroxine rings of COF-1 also function as the cross-linking points through the coordination bond between the lone pair of the nitrogen atom and vacant p-orbital of the boron atom.

Figure 9 shows the oxidation potential of SME/LiTFSA (Li/O = 0.17) in a LSV measurement. The electrochemical stability of electrolyte materials is an important factor for developing rechargeable batteries because electrolyte materials with wide electrochemical windows are required for high-voltage active materials such as $LiCoO_2$ and $LiNi_{1/3}Mn_{1/3}Co_{1/3}O_2$, but the oxidation potential of PEO-based electrolytes is only about 4 V vs. Li/Li$^+$. The LSV measurements indicated that SME/LiTFSA has good oxidation stability of 4.60 V vs. Li/Li$^+$, which is higher than that of PEO-based electrolytes, at a current density of 0.10 μA cm^{-1}. Yoshida et al. (2011) reported that an electron pair of ether oxygen is partially donated to the Lewis acidic cation (Li$^+$) leading to a decrease of the HOMO level of oligoether compounds. Therefore, the electrochemical window is widened.

Figure 10 shows the first hundred cycles in the CVs for SME/LiTFSA on pristine Ni electrodes at 60°C. The voltammograms of the SME/LiTFSA electrolyte shows a reduction peak at 0.42 V and an oxidation peak at 0.82 V.

These reduction and oxidation peaks are probably associated with a redox process involving electrode surface species, such as oxides (Abraham et al., 1997). In addition, the solid SME/LiTFSA composite showed a reduction peak for Li^+ at about −0.2 V vs. Li/Li^+ and an oxidation peak for Li at about 0.1 V vs. Li/Li^+ over 100 cycles. The electrochemical stability of SME/LiTFSA composites is acceptable toward Li metal. Interestingly, the current density of stripping/plating reactions of Li increased with increasing the number of cycle during 100 cycles. The SME/LiTFSA composite exhibited stable and reversible stripping/plating reactions of Li, indicating that SME functions as a Li-ion conductor.

CONCLUSION

This study developed novel SMEs by the formation of a cross-linking network based on ED-2003 with amines on both chain ends and COF-1 with a two-dimensional boroxine skeleton. The structure of COF-1, ED-2003, and their composites was investigated by various techniques. The crystallinity of COF-1 and ED-2003 was inhibited by mixing, and SME was obtained as an amorphous compound with a low T_g of −56°C, which is superior as an ion conductive matrix. The T_g values of SME/LiTFSA composites monotonously increased with increasing Li salt concentration due to the interaction between ether units and Li^+. The ionic conductivity also increased with increasing Li salt concentration and reached a maximum value at Li/O = 0.17, which is a higher concentration than those of polyether and its derivatives. Boroxine rings will contribute to the dissociation of LiTFSA and produce a large amount of ions in the matrix through the interaction between anion and boroxine rings. SME/LiTFSA (Li/O = 0.17) showed the t_{Li+} of 0.34 at 60°C, which was higher than those of PEO/LiTFSA. The boroxine rings of COF-1 functioned as anion receptor sites through the coordination bond between electron-rich anion and vacant p-orbital of boron atom. SME/LiTFSA composites exhibited reversible striping/plating reactions of Li over 100 cycles. These results revealed that SME functions as a Li-ion conductor and will be a new concept to develop SPEs for rechargeable batteries.

DATA AVAILABILITY STATEMENT

The original contributions presented in the study are included in the article/supplementary material, further inquiries can be directed to the corresponding author/s.

AUTHOR CONTRIBUTIONS

SH and MY-F designed the research. SH, TU, and JI prepared the samples and measured the properties. YT, MR, and MY-F participated in the data analysis. SH and MY-F wrote the manuscript. All authors contributed to the article and approved the submitted version.

FUNDING

This study was supported by a Grant-in-Aid for Scientific Research (C) (No. 26410140) from the Japan Society for the Promotion of Science (JSPS).

REFERENCES

Abraham, K. M., Jiang, Z., and Carroll, B. (1997). Highly conductive PEO-like polymer electrolytes. *Chem. Mater.* 9, 1978–1988. doi: 10.1021/cm970075a

Agrawal, R. C., and Pandey, G. P. (2008). Solid polymer electrolytes: materials designing and all-solid-state battery applications: an overview. *J. Phys. D Appl. Phys.* 41:223001. doi: 10.1088/0022-3727/41/22/223001

Appetecchi, G. B., Croce, F., Hassoun, J., Scrosati, B., Salomon, M., and Cassel, F. (2003). Hot-pressed, dry, composite, PEO-based electrolyte membranes: I. ionic conductivity characterization. *J. Power Sourc.* 114, 105–112. doi: 10.1016/s0378-7753(02)00543-8

Appetecchi, G. B., Henderson, W., Villano, P., Berrettoni, M., and Passerini, S. (2001). PEO-LiN(SO[sub 2]CF[sub 2]CF[sub 3])[sub 2] Polymer Electrolytes: i. XRD, DSC, and ionic conductivity characterization. *J. Electrochem. Soc.* 148:A1171.

Appetecchi, G. B., Shin, J. H., Alessandrini, F., and Passerini, S. (2005). 0.6Ah Li/V2O5 battery prototypes based on solvent-free PEO–LiN(SO2CF2CF3)2 polymer electrolytes. *J. Power Sourc.* 143, 236–242. doi: 10.1016/j.jpowsour.2004.11.039

Armand, M., and Tarascon, J. M. (2008). Building better batteries. *Nature* 451, 652–657. doi: 10.1038/451652a

Armand, M. B. (1986). Polymer electrolytes. *Ann. Rev. Mater. Sci.* 16, 245–261.

Côté, A. P., Benin, A. I., Ockwig, N. W., Keeffe, M., Matzger, A. J., and Yaghi, O. M. (2005). Porous, crystalline, covalent organic frameworks. *Science* 310:1166. doi: 10.1126/science.1120411

Côté, A. P., El-Kaderi, H. M., Furukawa, H., Hunt, J. R., and Yaghi, O. M. (2007). Reticular synthesis of microporous and mesoporous 2D covalent organic frameworks. *J. Am. Chem. Soc.* 129, 12914–12915.

Dienstmaier, J. F., Gigler, A. M., Goetz, A. J., Knochel, P., Bein, T., Lyapin, A., et al. (2011). Synthesis of well-ordered cof monolayers: surface growth of nanocrystalline precursors versus direct on-surface polycondensation. *ACS Nano* 5, 9737–9745. doi: 10.1021/nn2032616

Du, Y., Calabro, D., Wooler, B., Li, Q., Cundy, S., Kamakoti, P., et al. (2014). Kinetic and mechanistic study of COF-1 phase change from a staggered to eclipsed model upon partial removal of mesitylene. *J. Phys. Chem. C* 118, 399–407. doi: 10.1021/jp4097293

Du, Y., Mao, K., Kamakoti, P., Wooler, B., Cundy, S., Li, Q., et al. (2013). The effects of pyridine on the structure of B-COFs and the underlying mechanism. *J. Mater. Chem. A* 1, 13171–13178. doi: 10.1039/c3ta12515g

Eriksson, T., Mace, A., Manabe, Y., Yoshizawa-Fujita, M., Inokuma, Y., Brandell, D., et al. (2020). Polyketones as host materials for solid polymer electrolytes. *J. Electrochem. Soc.* 167:070537. doi: 10.1149/1945-7111/ab7981

Evans, J., Vincent, C. A., and Bruce, P. G. (1987). Electrochemical measurement of transference numbers in polymer electrolytes. *Polymer* 28, 2324–2328. doi: 10.1016/0032-3861(87)90394-6

Feng, S., Shi, D., Liu, F., Zheng, L., Nie, J., Feng, W., et al. (2013). Single lithium-ion conducting polymer electrolytes based on poly[(4-styrenesulfonyl)(trifluoromethanesulfonyl)imide] anions. *Electrochim. Acta* 93, 254–263. doi: 10.1016/j.electacta.2013.01.119

Karan, N. K., Pradhan, D. K., Thomas, R., Natesan, B., and Katiyar, R. S. (2008). Solid polymer electrolytes based on polyethylene oxide and lithium trifluoro- methane sulfonate (PEO–LiCF3SO3): ionic conductivity and dielectric relaxation. *Solid State Ion.* 179, 689–696. doi: 10.1016/j.ssi.2008.04.034

Klontzas, E., Tylianakis, E., and Froudakis, G. E. (2010). Designing 3D COFs with enhanced hydrogen storage capacity. *Nano Lett.* 10, 452–454. doi: 10.1021/nl903068a

Lanni, L. M., Tilford, R. W., Bharathy, M., and Lavigne, J. J. (2011). Enhanced hydrolytic stability of self-assembling alkylated two-dimensional covalent organic frameworks. *J. Am. Chem. Soc.* 133, 13975–13983. doi: 10.1021/ja203807h

Lascaud, S., Perrier, M., Vallee, A., Besner, S., Prud'homme, J., and Armand, M. (1994). Phase diagrams and conductivity behavior of poly(ethylene oxide)-molten salt rubbery electrolytes. *Macromolecules* 27, 7469–7477. doi: 10.1021/ma00103a034

Lei, Z., Yang, Q., Xu, Y., Guo, S., Sun, W., Liu, H., et al. (2018). Boosting lithium storage in covalent organic framework via activation of 14-electron redox chemistry. *Nat. Commun.* 9:576.

Li, C., Liu, L., Kang, J., Xiao, Y., Feng, Y., Cao, F.-F., et al. (2020). Pristine MOF and COF materials for advanced batteries. *Energy Storage Mater.* 31, 115–134. doi: 10.1016/j.ensm.2020.06.005

Liang, W.-J., Chen, T.-Y., and Kuo, P.-L. (2004). Solid polymer electrolytes. VII. preparation and ionic conductivity of gelled polymer electrolytes based on poly(ethylene glycol) diglycidyl ether cured with α,ω-diamino poly(propylene oxide). *J. Appl. Polym. Sci.* 92, 1264–1270. doi: 10.1002/app.13716

Magistris, A., Mustarelli, P., Quartarone, E., and Tomasi, C. (2000). Transport and thermal properties of (PEO)n–LiPF6 electrolytes for super-ambient applications. *Solid State Ion.* 13, 1241–1247. doi: 10.1016/s0167-2738(00)00594-4

Marzantowicz, M., Dygas, J. R., Krok, F., Łasińska, A., Florjańczyk, Z., Zygadło-Monikowska, E., et al. (2005). Crystallization and melting of PEO:LiTFSI polymer electrolytes investigated simultaneously by impedance spectroscopy and polarizing microscopy. *Electrochim. Acta* 50, 3969–3977. doi: 10.1016/j.electacta.2005.02.053

Matsumi, N., Nakashiba, M., Mizumo, T., and Ohno, H. (2005). Novel polymer/salt hybrid composed of comblike organoboron polymer electrolyte and boron-stabilized imido anion. *Macromolecules* 38, 2040–2042. doi: 10.1021/ma047469p

Matsumi, N., Sugai, K., and Ohno, H. (2003). Ion conductive characteristics of alkylborane type and boric ester type polymer electrolytes derived from mesitylborane. *Macromolecules* 36, 2321–2326. doi: 10.1021/ma021734u

Mehta, M. A., Fujinami, T., and Inoue, T. (1999). Boroxine ring containing polymer electrolytes. *J. Power Sourc.* 8, 724–728. doi: 10.1016/s0378-7753(99)00151-2

Meyer, W. H. (1998). Polymer electrolytes for lithium-ion batteries. *Adv. Mater.* 10, 439–448.

Mindemark, J., Lacey, M. J., Bowden, T., and Brandell, D. (2018). Beyond PEO—Alternative host materials for Li+-conducting solid polymer electrolytes. *Prog. Polym. Sci.* 81, 114–143. doi: 10.1016/j.progpolymsci.2017.12.004

Okumura, T., and Nishimura, S. (2014). Lithium ion conductive properties of aliphatic polycarbonate. *Solid State Ion.* 267, 68–73. doi: 10.1016/j.ssi.2014.09.011

Pucić, I., and Jurkin, T. (2012). FTIR assessment of poly(ethylene oxide) irradiated in solid state, melt and aqeuous solution. *Radiat. Phys. Chem.* 81, 1426–1429. doi: 10.1016/j.radphyschem.2011.12.005

Ratner, M. A., and Shriver, D. F. (1988). Ion transport in solvent-free polymers. *Chem. Rev.* 88, 109–124. doi: 10.1021/cr00083a006

Smith, M. K., and Northrop, B. H. (2014). vibrational properties of boroxine anhydride and boronate ester materials: model systems for the diagnostic characterization of covalent organic frameworks. *Chem. Mater.* 26, 3781–3795. doi: 10.1021/cm5013679

Sun, B., Mindemark, J., Edström, K., and Brandell, D. (2014). Polycarbonate-based solid polymer electrolytes for Li-ion batteries. *Solid State Ion.* 262, 738–742. doi: 10.1016/j.ssi.2013.08.014

Tien, C.-P., Liang, W.-J., Kuo, P.-L., and Teng, H.-S. (2008). Electric double layer capacitors with gelled polymer electrolytes based on poly(ethylene oxide) cured with poly(propylene oxide) diamines. *Electrochim. Acta* 53, 4505–4511. doi: 10.1016/j.electacta.2008.01.021

Tominaga, Y., and Yamazaki, K. (2014). Fast Li-ion conduction in poly(ethylene carbonate)-based electrolytes and composites filled with TiO2 nanoparticles. *Chem. Commun. (Camb)* 50, 4448–4450. doi: 10.1039/c3cc49588d

Watanabe, M., Nagano, S., Sanui, K., and Ogata, N. (1988). Estimation of Li+ transport number in polymer electrolytes by the combination of complex impedance and potentiostatic polarization measurements. *Solid State Ion.* 2, 911–917. doi: 10.1016/0167-2738(88)90303-7

Wen, S. J., Richardson, T. J., Ghantous, D. I., Striebel, K. A., Ross, P. N., and Cairns, E. J. (1996). FTIR characterization of PEO + LiN(CF3SO2)2 electrolytes. *J. Electroanal. Chem.* 408, 113–118. doi: 10.1016/0022-0728(96)04536-6

Yang, H., Zhang, S., Han, L., Zhang, Z., Xue, Z., Gao, J., et al. (2016). High conductive two-dimensional covalent organic framework for lithium storage with large capacity. *ACS Appl. Mater. Interfaces* 8, 5366–5375. doi: 10.1021/acsami.5b12370

Yoshida, K., Nakamura, M., Kazue, Y., Tachikawa, N., Tsuzuki, S., Seki, S., et al. (2011). Oxidative-stability enhancement and charge transport mechanism in glyme–lithium salt equimolar complexes. *J. Am. Chem. Soc.* 133, 13121–13129. doi: 10.1021/ja203983r

Yue, L., Ma, J., Zhang, J., Zhao, J., Dong, S., Liu, Z., et al. (2016). All solid-state polymer electrolytes for high-performance lithium ion batteries. *Energy Storage Mater.* 5, 139–164.

Zhang, H., Liu, C., Zheng, L., Xu, F., Feng, W., Li, H., et al. (2014). Lithium bis(fluorosulfonyl)imide/poly(ethylene oxide) polymer electrolyte. *Electrochim. Acta* 133, 529–538. doi: 10.1016/j.electacta.2014.04.099

Conflict of Interest: The authors declare that the research was conducted in the absence of any commercial or financial relationships that could be construed as a potential conflict of interest.